Supporting Information

Activation-free fabrication of high-surface-area porous carbon nanosheets from conjugated copolymers

Youchen Tang,‡ Shaohong Liu,‡ Bingna Zheng, Ruliang Liu, Ruowen Fu, Dingcai Wu,* Mingqiu Zhang* and Minzhi Rong*

Materials Science Institute, PCFM Lab and GDHPRC Lab, School of Chemistry, Sun Yat-sen University, Guangzhou 510275, P.R. China.

E-mail: wudc@mail.sysu.edu.cn; ceszmq@mail.sysu.edu.cn; cesrmz@mail.sysu.edu.cn

EXPERIMENTAL

2 mL of GO aqueous solution (C6G6 Technology Co. Ltd.; 10 mg mL^{-1}) was first added into 80 mL of deionized water, and then sonicated for 1 h to achieve single layer GO aqueous dispersion. Subsequently, 0.216 mL of predistilled aniline and 0.164 mL of predistilled pyrrole were added with further sonication at room temperature for 1 h, followed by refluxing at 95 °C for 4h, leading to the formation of mrGO. After that, 1 g of ammonium persulfate aqueous solution and 0.1 mL of hydrochloric acid (12 M) were added into the above precooled suspension in sequence. The target product GO@PACP was then collected and washed with a large amount of deionized water after polymerization for 12 h at 0 °C. For the preparation of GO@PANi and GO@PPy samples, only 0.432 mL of aniline or 0.328 mL of pyrrole was added, respectively. GO/PACP was obtained without the modification process at 95 °C. PACP nanoparticles were obtained without the addition of GO.

GO@PACP, GO@PANi, GO@PPy, GO/PACP, and PACP were carbonized at 900 °C in N$_2$ flow for 15 h with a heating rate of 2 °C min^{-1}, leading to the formation

of HSA-PCNs-PACP, PCNs-PANi, PCNs-PPy, PCNs-PACP, and C-PACP, respectively. rGO was also obtained by treating GO under the same conditions.

The nanomorphologies were investigated with a field-emission scanning electron microscopy (FESEM, Hitachi S-4800), a transmission electron microscopy (TEM, Tecnai G2 Spirit), and an atomic force microscopy (AFM, Bruker Dimension edge). Pore structures were conducted on a Micromeritics ASAP 2020 analyser at 77 K. BET area surface and DFT pore size distribution were calculated based on Brunauer-Emmett-Teller theory and original Density Function Theory, respectively. FTIR spectra were provided by the Bruker Equinox 55. X-ray photoelectron spectroscopy (XPS) spectra were measured on a Thermo SCIENTIFIC ESCALAB 250Xi. Thermogravimetric analysis (TGA) was carried out on a TA Instruments Q50 at a heating rate of 10 $^{\circ}$C min^{-1} under nitrogen flow. X-ray diffraction (XRD) patterns were obtained on a RIGAKU D-MAX 2200 VPC with Cu-Kα radiation. Raman spectra were collected on a HORIBA JY with 532 nm lasers. The content of nitrogen in bulk was examined by a vario EL Elemental Analyzer (Elementar Germany).

Table S1. Comparison of S_{BET} between the HSA-PCNs-PACP sample and other previously reported graphene-templated porous carbon nanosheets.

Sample	Precursor	S_{BET} (m² g⁻¹)	Reference
HSA-PCNs-PACP	**PACP**	**1606**	**This work**
GNPCSs-800	ZIF-8	911	[S1]
GMP-S	thiophene-containing polymers	888	[S2]
NMCSs-11.6	resorcinol/formaidehyde polymers	791	[S3]
TPC	melamine /aromatic dialdehyde polymers	762	[S4]
NDCN-7	polydopamine	652	[S5]
CMP-2D	conjugated microporous polymers	593	[S6]
G-CBP-a	aniline, 3-aminophenylboronic acid, and m-phenylenediamine polymers	363	[S7]
N-RG-O	polyaniline and polypyrrole	350	[S8]
N-CNs	polydopamine	273	[S9]

Table S2. Summary of the pore parameters for different samples.

Sample	S_{BET} (m² g⁻¹)	S_{ext} (m² g⁻¹)	S_{mic} (m² g⁻¹)	V_{mic} (cm³ g⁻¹)	V_t (cm³ g⁻¹)
HSA-PCNs-PACP	1606	422	1184	0.51	1.01
PCNs-PACP	1377	285	1092	0.5	1.04
PCNs-PANi	1021	247	774	0.36	0.88
PCNs-PPy	350	180	170	0.08	1.08
C-PACP	1120	271	849	0.39	0.92
rGO	108	103	5	0.004	0.10

Note: S_{BET}, S_{ext}, S_{mic}, V_{mic}, V_t denote BET surface area, t-plot external surface area, micropore surface area, micropore volume, and total pore volume, respectively.
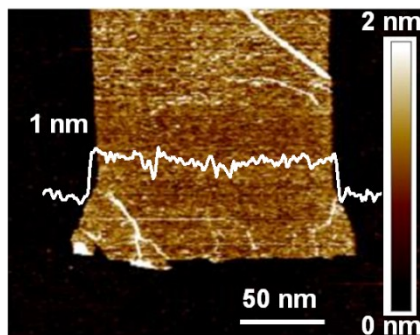
Fig. S1 AFM image of a GO nanosheet. The average thickness is determined to be 1 nm, suggesting the single layer characteristic of GO nanosheet.[S10]
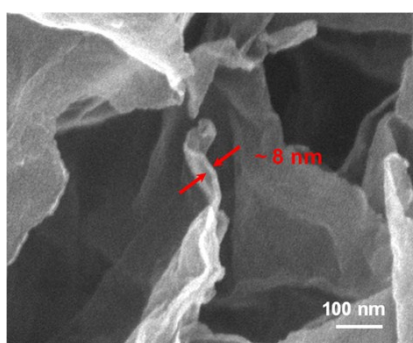
Fig. S2 SEM image of a GO@PACP nanosheet, showing a thickness of about 8 nm. This means the PACP coating is about 3.5 nm, since the GO thickness is about 1 nm (Fig. S1).
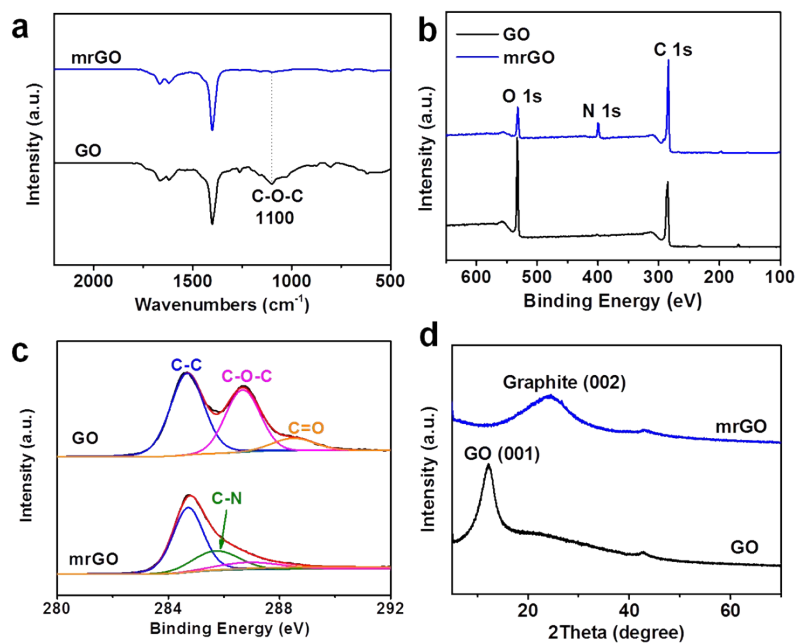
Fig. S3 (a) FTIR spectra, (b) XPS full scans, (c) high-resolution C 1s spectra, and (d) XRD patterns of GO and mrGO.
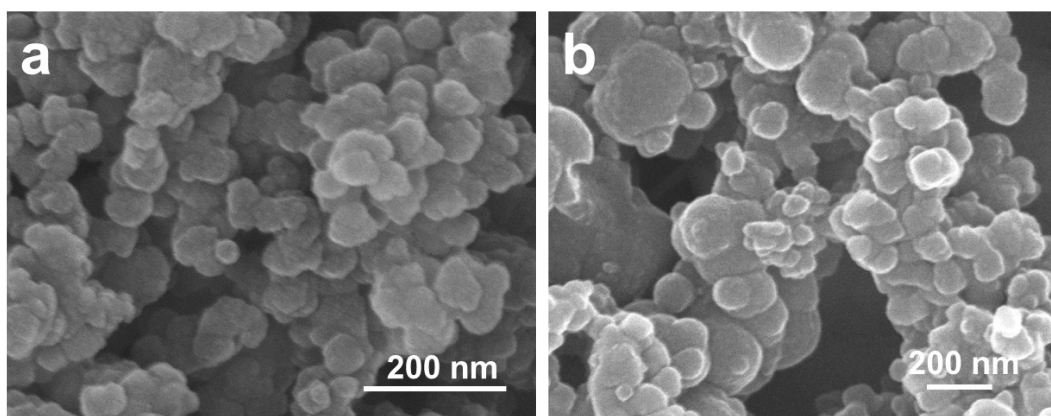
Fig. S4 SEM images of (a) PACP nanoparticles and (b) their carbonized product C-PACP prepared without GO templates.
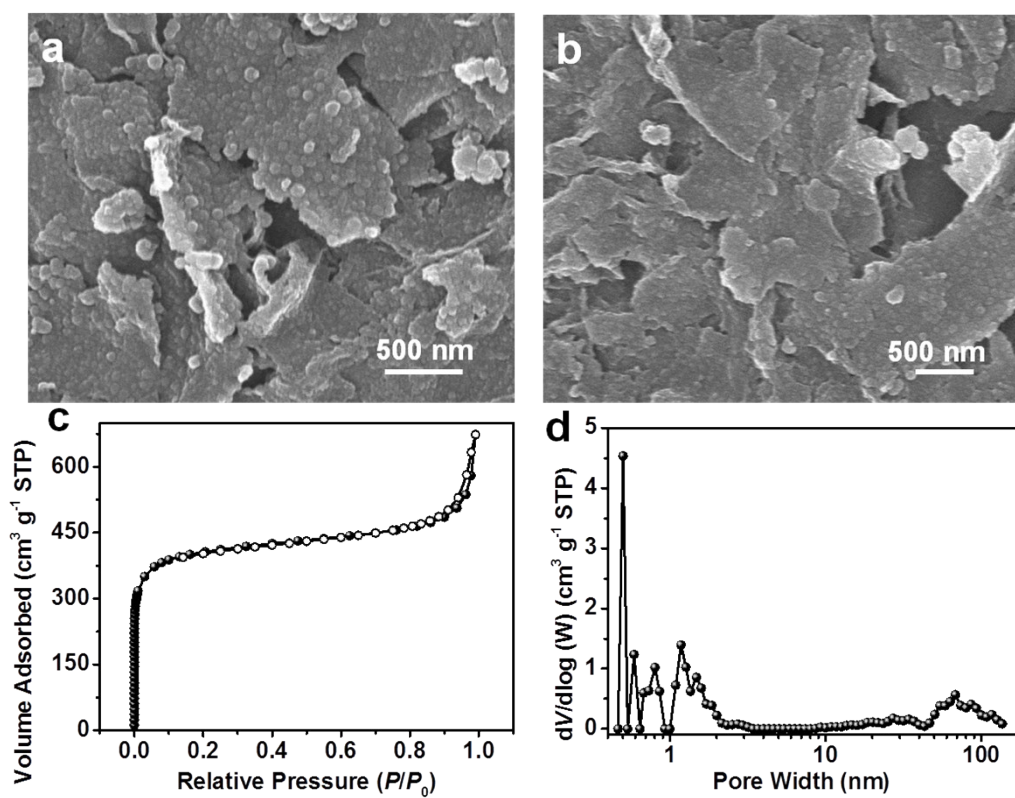
Fig. S5 SEM images of (a) GO/PACP and (b) its carbonized product PCNs-PACP. (c) N_2 adsorption–desorption isotherm and (d) DFT pore size distribution curve of PCNs-PACP.
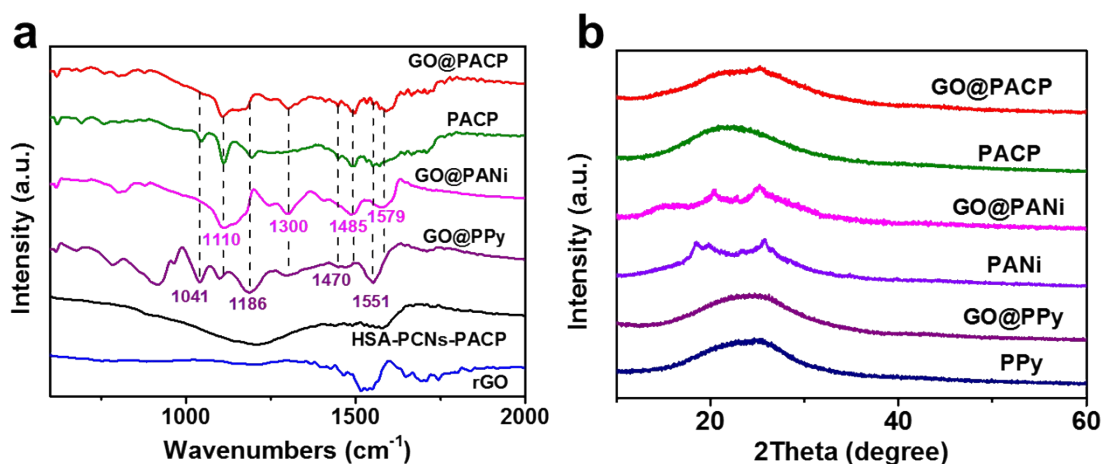
Fig. S6 (a) FTIR spectra of GO@PACP, PACP, GO@PANi, GO@PPy, HAS-PCNs-PACP and rGO. For GO@PANi, the bands at 1579, 1485, 1300 and 1100 cm^{-1} are attributed to the C=C stretch of quinoid and benzenoid rings, the C-N stretch and N=Q=N stretch of quinonoid ring, respectively. For GO@PPy, the bands at 1551 and 1470 cm^{-1} are assigned to the stretch of pyrrole ring, the band at 1186 cm^{-1} to the C-N stretch, the band at 1041 cm^{-1} to the C-H out of plane vibration, and the bands below 900 cm^{-1} to the C-H out of plane vibration. For PACP and GO@PACP, the bands at 1579, 1551, 1485, 1470, 1300, 1186, 1100 and 1041 cm^{-1} confirm the formation of PACP copolymers. Additionally, the band intensities of polypyrrole at 1551 and 1186 cm^{-1} decrease, some bands shift to low wavenumbers and more complicated bands appear in GO@PACP, indicating that PACP is successfully obtained instead of a simple mixture of PANi and PPy.[S11,S12] After carbonization, these bands disappear. (b) XRD patterns of GO@PACP, PACP, GO@PANi, PANi, GO@PPy and PPy. A broad band at intermediate positions (2θ = 24°) between those of PANi and PPy implies a low crystalline degree for PACP and thus a shorter conjugation length for PACP chains.
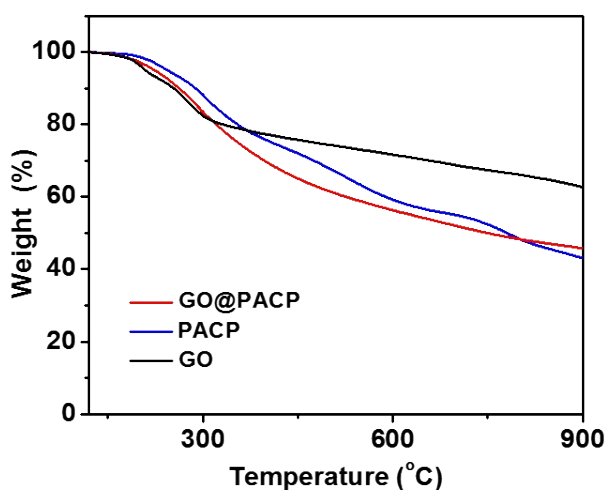
Fig. S7 TGA curves of GO, PACP and GO@PACP under nitrogen flow at a heating rate of 10 °C min^{-1}. The remaining weights of GO, PACP and GO@PACP at 900 °C are 63%, 43% and 46%, respectively.
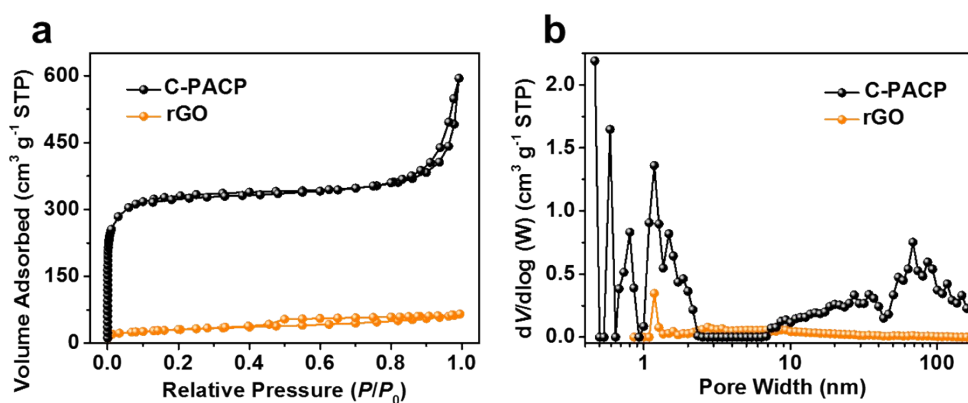
Fig. S8 (a) N_2 adsorption–desorption isotherms and (b) DFT pore size distribution curves of C-PACP and rGO.
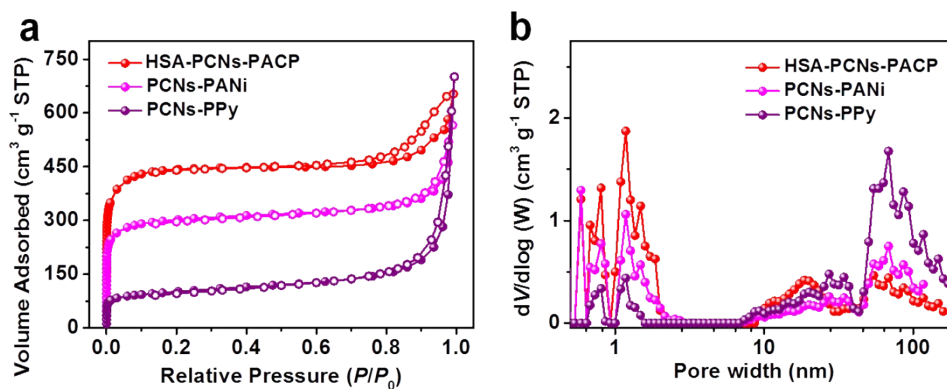
Fig. S9 (a) N_2 adsorption–desorption isotherms and (b) DFT pore size distribution curves of HSA-PCNs-PACP, PCNs-PANi and PCNs-PPy.
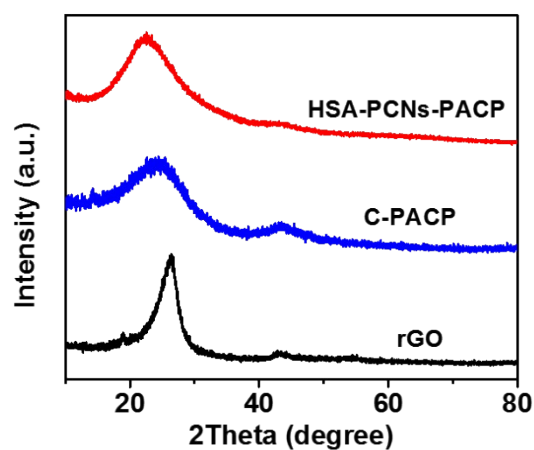
Fig. S10 XRD patterns of HSA-PCNs-PACP, C-PACP and rGO.
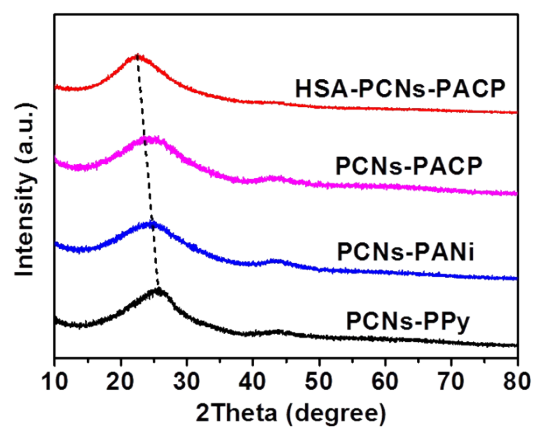
Fig. S11 XRD patterns of HSA-PCNs-PACP, PCNs-PACP, PCNs-PANi and PCNs-PPy.
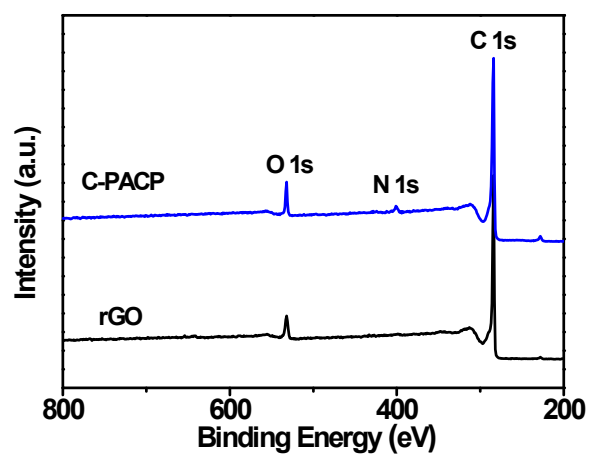
Fig. S12 XPS spectra of rGO and C-PACP. The content of N element for C-APCP is 3.5 at%, similar to that for HSA-PCNs-PACP.

References

S1. H.X. Zhong, J. Wang, Y.W. Zhang, W.L. Xu, W. Xing, D. Xu, Y.F. Zhang, X.B. Zhang, *Angew. Chem. Int. Ed.,* 2014, **53,** 14235-14239.

S2. X. Zhuang, F. Zhang, D. Wu, N. Forler, H. Liang, M. Wagner, D. Gehrig, M. R. Hansen, F. Laquai and X. Feng, *Angew.Chem. Int. Ed.,* 2013, **52**, 9668-9672.

S3. Z. Y. Jin, A. H. Lu, Y. Y. Xu, J. T. Zhang and W. C. Li, *Adv. Mater.,* 2014, **26**, 3700-3705.

S4. X. Zhuang, F. Zhang, D. Wu and X. Feng, *Adv. Mater.,* 2014, **26**, 3081-3086.

S5. W. Wei, H. Liang, K. Parvez, X. Zhuang, X. Feng and K. Mullen, *Angew.Chem. Int. Ed.,* 2014, **53**, 1570-1574.

S6. X. Zhuang, D. Gehrig, N. Forler, H. Liang, M. Wagner, M. R. Hansen, F. Laquai, F. Zhang and X. Feng, *Adv. Mater.,* 2015, **27**, 3789-3796.

S7. Y. Zhang, X. Zhuang, Y. Su, F. Zhang and X. Feng, *J. Mater. Chem.*, 2014, **2**, 7742.

S8. L. Lai, J. R. Potts, D. Zhan, L. Wang, C. K. Poh, C. Tang, H. Gong, Z. Shen, J. Lin and R. S. Ruoff, *Environ. Sci. Technol.*, 2012, **5**, 7936.

S9. K. Qu, Y. Zheng, S. Dai and S. Z. Qiao, *Nano Energy,* 2016, **19**, 373-381.

S10. C. Z. Zhu, S. J. Guo, Y. X. Fang and S. J. Dong, *ACS Nano*, 2010, **4**, 2429-2437.

S11. V. Lim, E. Kang, K. Neoh, Z. Ma, and K. Tan, *Appl. Surf. Sci.,* 2001, **181**, 317-326.

S12. B. L. Liang, Z. Y. Qin, T. Li, Z. J. Dou, F. X. Zeng, Y. M. Cai, M. F. Zhu, and Z. Zhou, *Electrochim. Acta,* 2015, **177**, 335-342.